

# Enhancement of solar panel power generation performance with a passive sun tracking system

Guoyang Song<sup>1</sup>, Defa Han<sup>2</sup>, Yingge Li<sup>1,2</sup>, Zhaoming He<sup>3</sup>, Dongxing Du<sup>1,\*</sup>

<sup>1</sup> Geo-Energy Research Institute, College of Electromechanical Engineering, Qingdao University of Science and Technology, Qingdao 266100, China

<sup>2</sup> College of Automation and Electronic Engineering, Qingdao University of Science and Technology, Qingdao 266100, China

<sup>3</sup> Department of Mechanical Engineering, Texas Tech University, Lubbock TX 79409, USA

\* **Corresponding author:** Dongxing Du, [du-dongxing@qust.edu.cn](mailto:du-dongxing@qust.edu.cn)

## CITATION

Song G, Han D, Li Y, et al.  
Enhancement of solar panel power generation performance with a passive sun tracking system.  
Thermal Science and Engineering. 2024; 7(1): 7906.  
<https://doi.org/10.24294/tse.v7i1.7906>

## ARTICLE INFO

Received: 12 February 2024  
Accepted: 9 March 2024  
Available online: 20 March 2024

## COPYRIGHT



Copyright © 2024 by author(s).  
Thermal Science and Engineering is published by EnPress Publisher, LLC. This work is licensed under the Creative Commons Attribution (CC BY) license.  
<https://creativecommons.org/licenses/by/4.0/>

**Abstract:** In this paper, a solar tracking device that can continuously track the sun by adjusting the direction and angle of the solar panel in real time is designed and fabricated to improve the power generation efficiency of the solar cell panel. The mechanical parts as well as the automatic control part of the passive sun-tracking system are described, and the efficiency enhancement with the sun-tracking solar panel is characterized in comparison with the fixed panel system. The test results show that in the spring season in Qingdao city of eastern China, the sun-tracking system can improve the solar cell power generation efficiency by 28.5%–42.9% when comparing to the direction and elevation angle fixed system in sunny days. Even in partly cloudy days, the PV power output can be increased by 37% with using the passive sun-tracking system. Economic analysis results show the cost-benefit period is about 10 years, which indicates that the passive sun tracking device can substantially contribute to the solar energy harvest practices.

**Keywords:** solar cell panel; passive sun-tracking system; design; fabrication; power generation efficiency

## 1. Introduction

Global population growth and economic development have led to a continuous increase in energy demand. Accompanying the rapid growth of energy consumption, the CO<sub>2</sub> concentration in the atmosphere has increased from 300 ppm before the industrial revolution to the current 410 ppm [1], and climate change has arisen as a major concern of the human society. The technologies on reducing and controlling the greenhouse gas emissions, therefore, have become one of the most attractive research aspects in recent years [2–11]. Many countries are accelerating the development and utilization of clean energy to reduce their dependence on fossil fuels to achieve the lower greenhouse gas emission goals. Under such circumstances, solar photovoltaic (PV) energy, which stands as one of the most prominent alternatives in emerging clean energies, has been quickly developed. Abundantly and widely distributed in almost all the world regions, clean and renewable solar power is expected to become an economically viable energy choice when compared to the traditional fossil fuel-based electricity generation industry [12–22].

With the development of solar energy technology and the realization of economies of scale, the cost of solar power generation continues to decrease. At present most solar panel systems are fixed installations on home roofs and other locations [23–25]. Due to the fixed orientation, these solar panels have a power

generation efficiency as low as 7% [26]. To enhance the efficiency of solar panels, solar tracking concept was proposed to keep the solar panels always aligned with the sun, therefore to achieve maximal efficiency and power generation [27]. In general, solar tracking can be accomplished through two methods: 1) single-axis solar tracking systems, and 2) dual-axis solar tracking systems [28,29]. The dual-axis solar tracking systems has shown obvious superiors to the single-axis systems on energy collection efficiency as well as on the system adaptability to various geographical and climatic conditions.

Dual-axis systems allow solar panels to adjust in two directions (horizontal and vertical), thus enabling precise tracking of the sun's position to maintain optimal perpendicular alignment with sunlight throughout the day, and maximizing electricity generation efficiency. Mpodu et al. [30] reviewed studies concerning the dual-axis photovoltaic tracking systems and reported the dual-axis system can increase electricity generation by 30%–40% and by adjusting angles, dual-axis systems mitigate shading effects from nearby buildings or obstacles. Josely Jose et al. [31] produced a small scale automated solar ray tracking device, and studied solar radiation and PV parameters using spectral, PV panel and LDR (Light Dependent Resistor) sensors characterization techniques. Their results indicated the maximum energy can be achieved with the solar tracking system. Zaghba et al. [32] conducted simulation and experimental assessment works concerning the outdoor performance of the PV systems in a 11.28 kWp grid, and reported that the dual-axis solar tracking system could achieve the greatest performance improvement of 20.89%. They further compared the mitigation amount of CO<sub>2</sub> among three installation managements of the stationary PV system, one axis PV system, and the dual-axis tracking PV systems, and reported the largest value of 5.85 tons in dual-axis system against 4.84 tons and 5.46 tons in other two systems. Mamodiya and Tiwari [28] constructed a closed-loop real-life solar tracking system consisting of a mechanical and electrical system based on the Simulink and Solidworks platform, and reported the sufficient strength as well as the enhanced effectiveness of the solar PV system. Muthukumar et al. [33] proposed a dual-axis solar track system and monitored the energy output data in 24 h at the interval of 0.2 s to validate the robustness of the system. They concluded the dual-axis system is an effective but inexpensive way to improve the solar energy output efficiency.

On the other hand, although solar tracking systems can improve the power generation efficiency, the power consumption associated with the solar tracking motion will increase by at least 20% to 30% compared to fixed solar panel arrangements [34]. Awasthi et al. [35] discussed various types of solar photovoltaic systems and solar tracking systems, focusing on recent advancements in dual-axis tracking system design and performance. They pointed out the drawbacks of dual-axis solar systems, such as expensive sensor costs and structural complexity. To address these negative issues, Boukdir and EL Omari [36] designed a novel dual-axis system with three LDR sensors, two LDRs for the azimuthal tracking while the other one for the elevation tracking, to achieve the high precision tracking operation. They tried to balance between sun tracking precision and cost, however their system still require improvements to cope with the adverse weather conditions. Palomino-Resendiz et al. [37] introduced a Model Predictive Controller (MPC) to the two-axis

solar tracing system, and performed numerical and experimental validation works on the improved performance on energy consumption during the solar tracker operation. Their results showed the MPC could reduce the energy consumption of 90% average however at higher tracking error. Lu and Ajay [38] proposed a novel solar sensor based sun tracking system to balance the precise tracking movements and the PV energy production. They developed a Proportional-Integral-Derivative (PID) controller and employed Algorithm Optimization (AO) to minimize the energy cost in panel movement and thus increase the system capacity on the solar energy harvesting. Anshory et al. [39] utilized ESP8266 microcontroller to control the PV panel movement following the sunlight information from a LDR sensor. Based on the measurement data of current, voltage and temperature, they concluded their new design could increase the system response sensitivity, panel movement accuracy, and the energy harvest efficiency in comparison to the manual control system. Based on above literature review works, it is found there is still a current need for the dual-axis sun tracking systems to achieve high efficiency on sun power harvest practices at the base of low power consumption and simple structure.

In this paper, we designed and fabricated a passive dual-axis solar tracking system based on the LDR sensor. The LDR receives and transmits the sun light signals to guide the low power motor to drive the solar panel in two ways, rotating and tilting, to accurately track the position of the sun. The two-way movement ensures that the solar panel could always be oriented toward the direction of maximum light intensity and therefore maximize its power generation efficiency. With the fabricated passive sun tracking system, we tested the power generation characteristics of sun-tracking solar panels under different weather conditions in the spring season in eastern China based on daily power generation records. To show the advantage of the passive sun-tracking system, we measured in comparison the power output of the fixed panel system and carried out economic analysis.

Accordingly, the paper is organized in the following sequences. In Chapter 2, the detailed descriptions on the mechanical parts as well as the control and measurement parts of the passive sun-tracking system were provided. In chapter 3, the sensitivity of the constructed apparatus was validated at the first place, then the measurements were performed in both sunny days and partly cloudy days to show the advantages of the sun tracking system over the fixed panel system in terms of the instantaneous power output and the cumulative daily power generation, furthermore economic advantages of the passive sun-tracking system were discussed by comparing with other reported systems with the similar functions. At last, the conclusions were presented in Chapter 4.

## **2. Passive sun tracking solar panel system**

### **2.1. Mechanical parts**

The solar cell panel employed in this study is a monocrystalline silicon panel with a specification size of  $1500 \times 640$  mm and a maximum output power of 110 W.

The physical installation diagram of the sun tracking device is shown in **Figure 1**. In accordance with the mechanical design requirements [40–42], the passive sun tracking system consists of the following mechanical structures: rotary support,

rotary bearing, solar panel support, base support, and screw rod slider module. The support parts of the tracking system are made of European standard  $30 \times 30$  aluminum alloy, with high strength and hardness but a relatively small density, which reduces the load on movement of the device. The threaded rod support plate uses a Q235-A steel plate with a thickness of 5 mm to improve the process scheme, ensuring its mechanical properties and assembly accuracy. The bearing part, on the other hand, employs slewing bearings that enable extensive rotation within confined spaces thus ensuring stability throughout the rotational process. Most importantly, these bearings exhibit lower energy requirements for rotational motion, thus could achieve overall energy savings on the mechanical movement of the sun-tracking system.

The detailed force analysis on the mechanical part of the dual-axis sun tracking system, which validates the strength as well as the stability of the system, is provided in section 3.1.

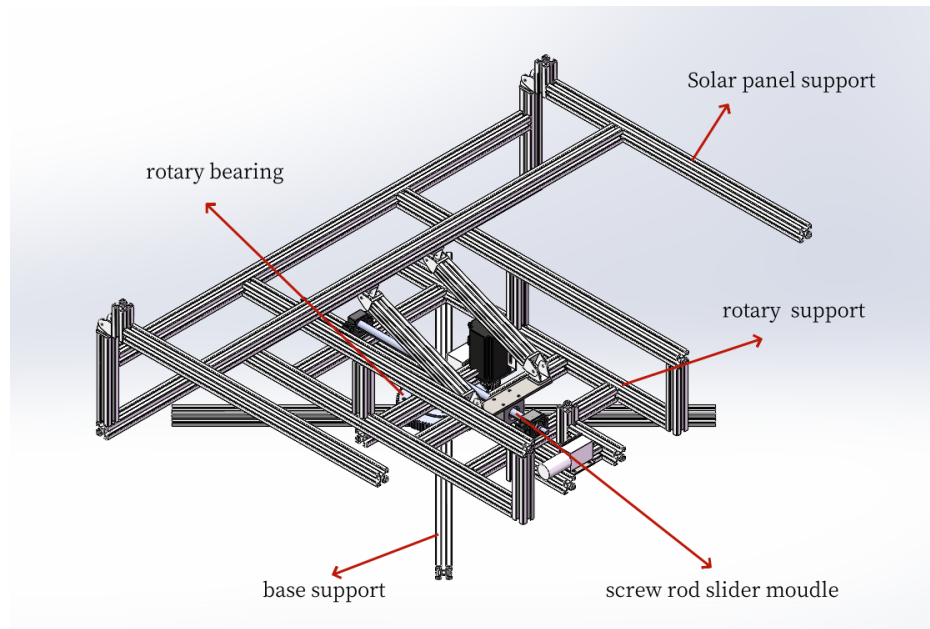


**Figure 1.** The mechanical parts installation diagram of the sun tracking system.

## 2.2. Control and measurement parts

The control and power output data collection parts incorporated in the physical system are depicted in **Figure 2**. As shown in the figure, the key parts of the automatic sun tracking system consist of an LDR sensor and a controller. The LDR sensor, which consists of two layer eight micro light sensors, converts the intensity of light into voltage and transmits the position information of the sun to the controller. The controller processes and analyzes the signals from the LDR sensor to determine the intensity and direction of sunlight. Then, the controller drives the worm gear reducer motor to turn the sun power panel until the panel aims exactly at the sun. The power consumption of the controller system is less than 5 W and can be well covered by the power generated by the sun panel, which means that as long as the system is set in sunlight circumstances, the controller would have enough power supply to operate automatically without an external power supply. The worm gear reducer motor functions at the rated voltage of 12 V and the maximum current of 3

A with a reduction ratio of 634 and is powered by the solar panel through the current regulator module. Under an unloaded speed of 3 r/min, the motor has an unloaded current of 0.1 A, while under a loaded speed of 2 r/min, the motor has a current of 0.9 A at a rated power of 10.8 W and a rated torque of 1.47 N · m.



**Figure 2.** Physical diagram of solar panel tracking device with light.

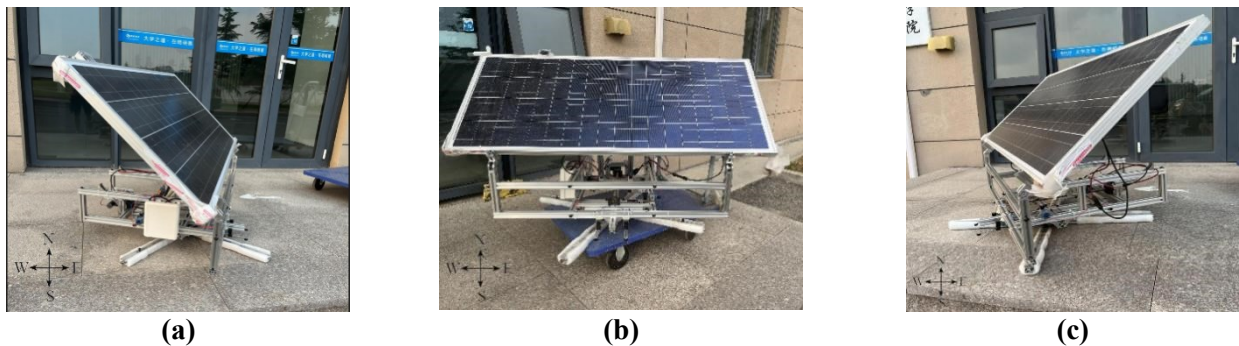


**Figure 3.** Operation state of the device in the (a) morning (7:30 am); (b) noon (12:00 am); (c) afternoon (5:00 pm) of the day.

**Figure 3a–c** show the operation status of the passive sun-tracking power panel system in the morning, noon and afternoon of a sunny day. It is observed the sun panel tracking system works automatically and precisely with a deviation angle of  $\leq 1^\circ$ .

To measure the instantaneous sun panel output, the Photovoltaic Panel Multimeter Tester (PPMT), a PVT801 model tester with a testing power range of 0–800 W, is integrated into the passive sun tracking system. Connected to the solar panel’s poles, the PPMT could monitor the instantaneous current and voltage output of the solar cell panel, thus measures the real-time maximum power generation capacity of the panel. By plotting the measured maximum power output at various times in the day, the power generation variation curve of the sun panel system could be obtained.

### 3. Results and analysis

#### 3.1. Stress analysis on the dual-axis sun tracking system

The strength and stability of the dual-axis sun tracking device is crucial for the safe and efficient performance of the system. In this section, force analysis was performed on the mechanical part of the system with help of the state-of-the-art ANSYS software. The finite element method is used to discretize the structure into a finite number of small element, and based on the force balance between the material internal forces and external loads, the stress distribution in the structure can be numerically obtained.

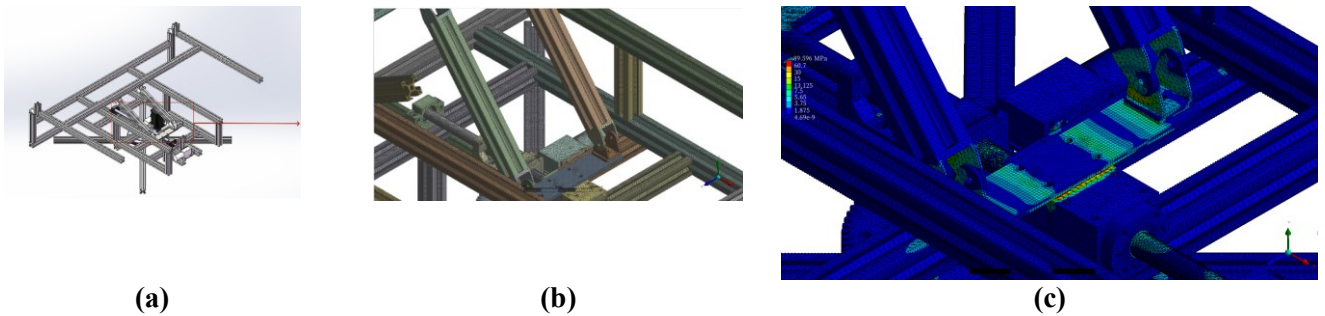


**Figure 4.** Force analysis of the mechanical part of the dual-axis sun-tracking system: (a) physical model; (b) meshing details; (c) stress distribution results.

**Figure 4a–c** displays the physical model of the mechanical part of the system, the mesh system as well as the stress distribution in the joint part of the apparatus after the force analysis study. In the stress analysis, a 200 N equivalent gravity force is applied above the solar panel support rod, and the device is subjected to a 2000 N wind load (about level 8 wind) in corresponding to the extreme weather conditions. As shown in **Figure 4c**, the simulation results indicate that the maximum stress occurs at the junction of the solar panel support bracket, with a maximum stress of 89.569 MPa, which is well below the yield strength 270 MPa and the tensile strength 310 MPa of the aluminum alloy material. The results indicate that the device's performance could meet the design requirements exceptionally well. It is observed the fabricated dual-axis sun tracking system exhibit high stability and load-bearing capacity under the harsh operational conditions and stress environments, thus ensuring the safe and reliable operation of the device in the practical applications.

#### 3.2. Test conditions for PV power output measurement

**Table 1** lists the dates when the measurements were performed. It is clearly observed that most days are sunny days, and 13th May and 21st, 22nd, 24th May, when it is slightly cloudy, cloudy, cloudy then sunny and cloudy then sunny, were employed to test the sensitivity of the measurement system.

**Table 1.** List of test dates and the weather conditions.

| <b>Date</b>   | <b>weather conditions</b> | <b>temperature</b> | <b>wind force scale</b> | <b>wind direction</b> |
|---------------|---------------------------|--------------------|-------------------------|-----------------------|
| 26 April 2023 | sunny                     | 11 °C–15 °C        | 4–5                     | southwest wind        |
| 1 May 2023    | sunny                     | 13 °C–18 °C        | 3–4                     | south wind            |
| 13 May 2023   | slightly cloudy           | 14 °C–20 °C        | 3–4                     | south wind            |
| 16 May 2023   | sunny                     | 18 °C–23 °C        | 3–4                     | south wind            |
| 21 May 2023   | cloudy                    | 15 °C–25 °C        | 3–4                     | northwest wind        |
| 22 May 2023   | cloudy then sunny         | 15 °C–23 °C        | 3–4                     | north wind            |
| 23 May 2023   | sunny                     | 18 °C–27 °C        | 3–4                     | northwest wind        |
| 24 May 2023   | cloudy then sunny         | 16 °C–18 °C        | 3                       | southeast wind        |

To reveal the enhancement of the power output with the passive sun-tracking system, tests were performed at the fixed solar panel position as the control group. In the fixed sun panel system, the sun panel always faces south at a certain lift angle to the ground. The optimal tilting angle varies with the region, with a larger optimal tilt angle for the larger latitude regions. Even in the same latitude region, the optimal tilt angle would be affected by local meteorological conditions and other factors, such as the radiation intensity differences in the proportion of scattered and direct radiation of the sun. Specifically, the optimal azimuth angle and tilt angle in Qingdao, where this experiment is performed, are azimuth angles 2°–3° west of due south and a tilt angle of 34° in the spring season. Therefore, as the control group of this experiment, an azimuth angle of 2° west of due south and a tilt angle of 34° were set for the fixed system tests.

In the measurement procedure, we firstly measure the power output of the solar panel in the sun-tracking position, then disconnect the control unit and manually adjust the panel support system to the fixed position to perform the controlled measurement. The data acquisition position and moment for two set of measurements are therefore deemed to be the same. In this manner, we could ensure the accurate comparisons on energy output results between the sun-tracking and the fixed solar panel system.

### **3.3. Sensitivity analysis of the sun panel power output**

Sensitivity studies of the sun panel power output in the passive sun-tracking system were performed on the 13th and 16th of May, as well as on the 21st–23rd of May, when the daily weather covers the slightly cloudy, cloudy & sunny to the all-day sunny conditions.

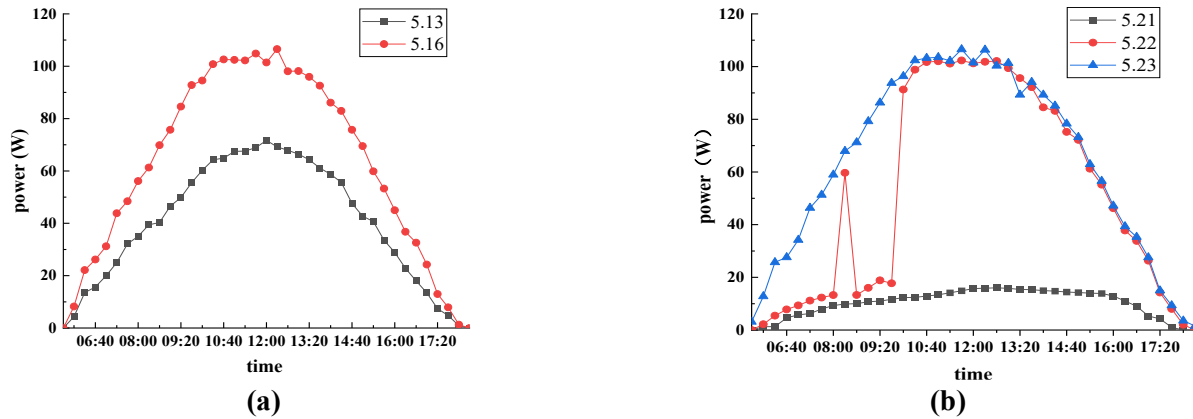


**Figure 5.** Sensitivity studies based on the solar panel power output comparisons under different weather conditions at **(a)** May 13th and 16th; **(b)** May 21st–23rd.

**Figure 5a** depicts the sun panel output on the slightly cloudy day of the 13th vs. on the sunny day of the 16th of May, whereas **Figure 5b** compares the sun panel output on three consecutive days, including the 21st a cloudy day, 22nd a cloudy then sunny day and 23rd a sunny day. It can be clearly observed from both subfigures that the sun panel shows satisfactory sensitivity to the sun radiation intensity, providing the highest power output on sunny days and giving the lowest power output on cloudy days. Its power generation varies sensitively with the different weather conditions as well. For instance, at 8:00–8:30 am in May 22nd, as shown in **Figure 5b**, the solar power output peak corresponds to the emerging sun from behind the clouds, whereas the sharp increasing on power curves around 10:00 am corresponds accurately to the weather change from cloudy to sunny in that day. Based on the results in **Figure 5**, the sensitivity of the passive solar energy system can be satisfactorily demonstrated.

### 3.4. Power generation enhancement of the passive sun-tracking system

Based on power output comparisons between the passive sun-tracking system and the fixed panel system at a tilting angle of  $34^\circ$  on various days with different weather conditions, the advantages of the power generation performance of the passive sun-tracking system could be clarified. **Figure 6a–d** compare the power output data in the four sunny days of April 26th, May 1st, 16th and 23rd, to reveal the significant difference in power generation efficiency between the passive sun tracking system and the fixed solar panel system under favorable weather conditions.

Based on the four subfigures of **Figure 6**, it is clearly observed that the power output data in the passive sun-tracking system are all remarkably higher than those of the fixed panel system, which indicates that the sun-tracking system can perform more efficiently than the always south-facing fixed panel system. In particular, a remarkable deviation in the power output curves appears in the morning and afternoon because the sun inclines toward the east and west in that period of the day, when the fixed panel system cannot face to the direct sunlight radiation, whereas the passive sun-tracking device can orient towards the sun thereby ensures the solar panel continuously receiving the high intensity sun radiation.

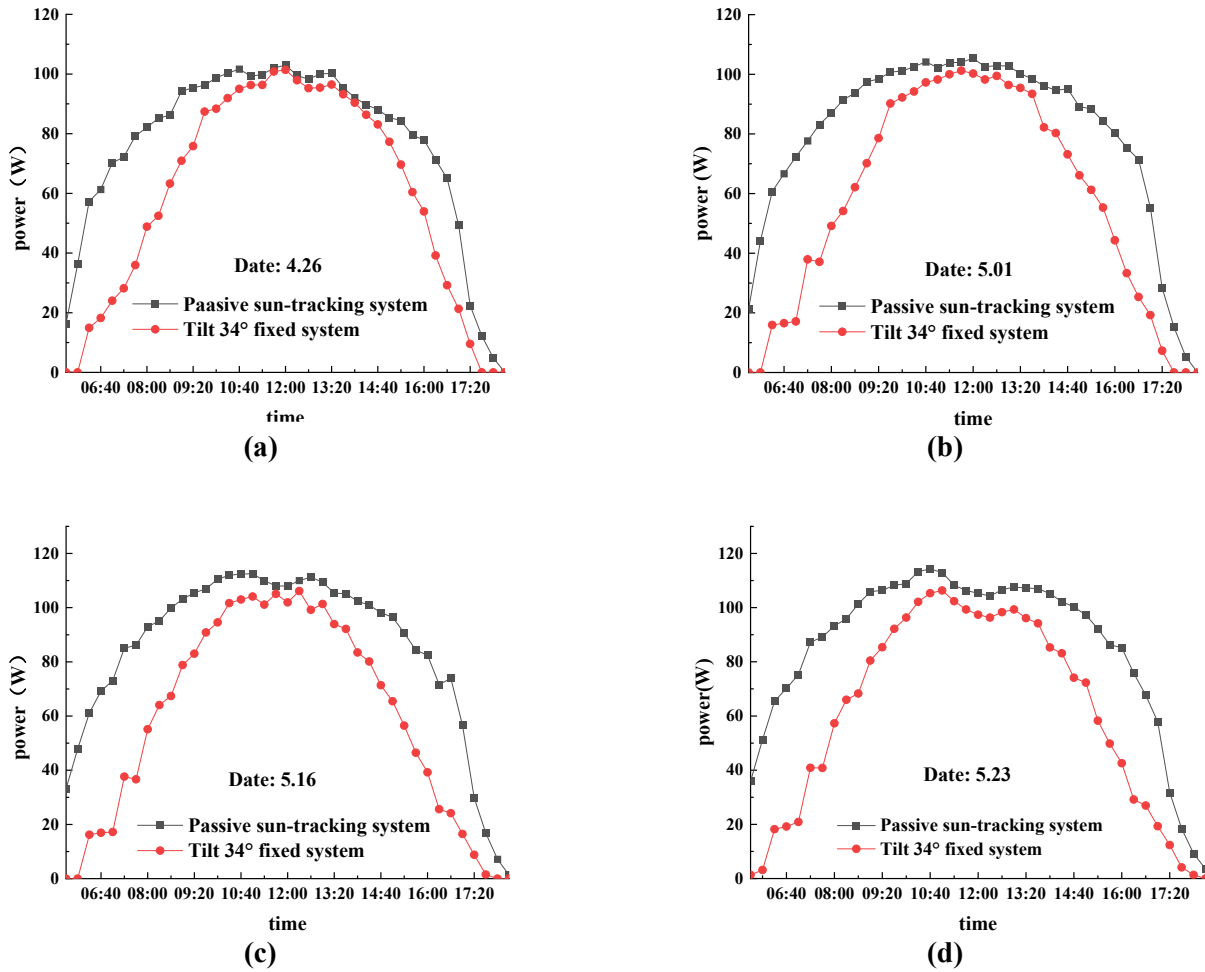


**Figure 6.** The daily power output results for both passive sun-tracking system and the fixed panel system at the sunny days of (a) April 26th; (b) May 1st; (c) May 16th; (d) May 23rd.

By integrating the instantaneous power output line over the time period of the day in **Figure 6a–d**, **Figure 7** plots the accumulative power output for the sun-tracking system and the fixed panel system at the aforementioned four sunny days. It is clearly observed the passive sun-tracking system can significantly elevate the daily power generation efficiency in comparison with the fixed panel system at a tilt angle of 34°. Specifically, as listed in **Table 2** in later part of the section, the exact extent of power output increase are in the range 29%–43%. In comparison with Alomar et al. [43], who reported the dual tracking system could yield extra energy up to 26% annually, the fabricated passive sun tracking system in this study has shown an even higher solar power generation efficiency.

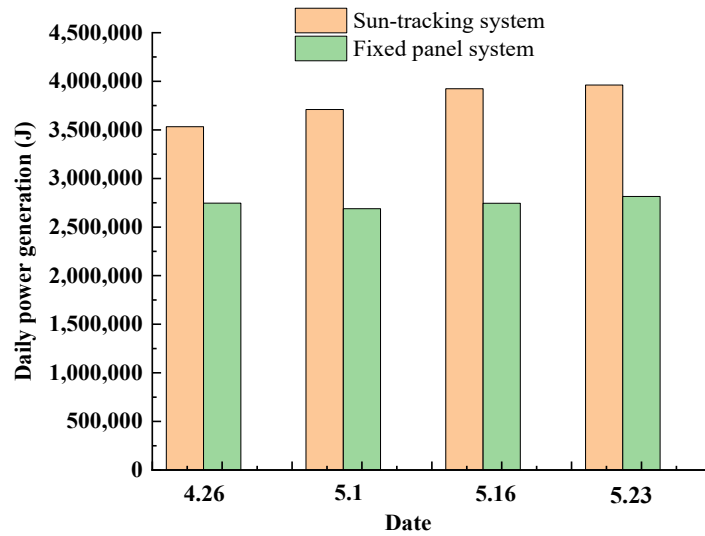


**Figure 7.** Comparisons on daily power output between the passive sun-tracking solar panel system and the fixed solar panel system at four sunny days.

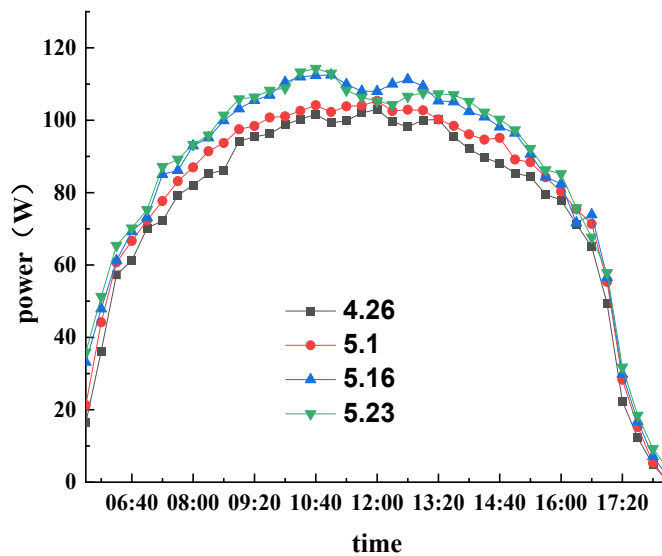


**Figure 8.** The power output curves of the passive sun-tracking system at various sunny days in the spring season showing the temperature effect.

In **Figure 7**, it is observed small difference in the output power of the fixed solar system among the few days, while the power output of the tracking solar system increases gradually with the change of date. The reason behind this observation can contribute to the different weather temperatures in these days. By referring to **Table 1**, it is observed the higher power output of the solar tracking system occurs at the date with higher weather temperature. **Figure 8** depicts the relationship between the weather temperatures and power output capacity of the passive sun-tracking solar panel system. In accordance to **Table 1**, the temperature on May 23rd is the highest at 18 °C–27 °C and the temperature on April 26th is the lowest at 11 °C–15 °C, the solar panel power output accordingly records the highest values on May 23rd and

the lowest values on April 26th. The power output from the fixed solar panel system shall be also sensible to the air temperature, however as shown in **Figure 6a–d**, the peak power output region of the fixed panel system only confines in the narrow mid noon period of the day, which restricts the favorable temperature effect on the daily power output of the fixed panel system.

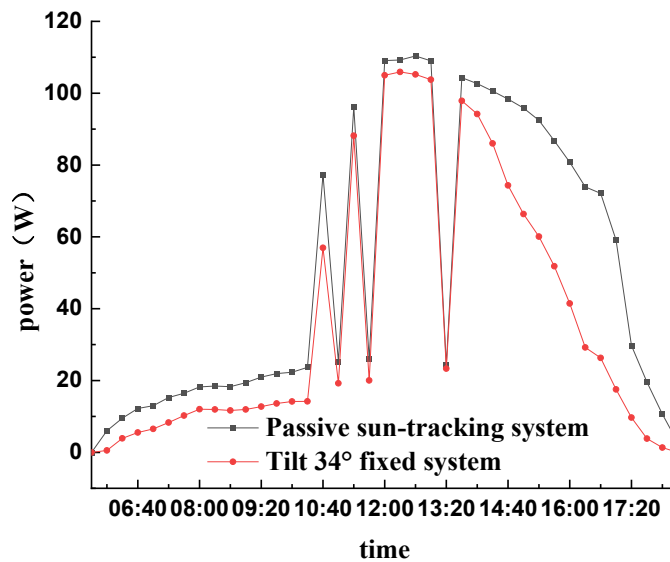


**Figure 9.** The daily power output result for both passive sun-tracking system and the fixed panel system at the cloudy and sunny day.

To check the robustness of the passive sun tracking system under unfavorable cloudy weather conditions, we conducted measurement in the date of May 24th, when the weather was cloudy and sunny. **Figure 9** plots the real time power output data of the sun tracking system together with those of the fixed panel system. The results clearly show that the power output levels under both configurations stayed at the low level under the cloudy condition at morning and noon, but returned to the optimal performance at the afternoon of that day when the weather turned into sunny. It is also found from **Figure 9** that the power output curves for both systems have the similar trends but the one for passive sun-tracking system is obviously higher than the solar PV panel fixed system. It is concluded the passive sun-tracking system show high sensitivity to the sun radiation even under the cloudy weather conditions and therefore enhances significantly the solar PV power generation efficiency.

**Table 2** summarizes the exact power generation outputs of the dual-axis sun tracking system and the fixed panel system in the aforementioned four sunny days and the one cloudy and sunny day. The power generation enhancement rates of the sun tracking system against the fixed panel system are also provided in the table. It is observed that, by employing the sun tracking system, the power generation capacity of the solar PV system could increase remarkably by 28.5%–42.9%, clearly showing the advantages of the passive dual-axis sun tracking system reported in this paper.

**Table 2.** Comparisons on the daily power generation results under different weather conditions between the sun-tracking system and the fixed panel system.

| Date and weather          | Power output of sun tracking system (J) | Power output of fixed system(J) | Enhancement rate |
|---------------------------|-----------------------------------------|---------------------------------|------------------|
| April 26 (sunny)          | 3,533,365.8                             | 2,746,718                       | 28.6%            |
| May 1 (sunny)             | 3,709,486.92                            | 2,689,351.2                     | 37.9%            |
| May 16 (sunny)            | 3,923,015.16                            | 2,744,821.2                     | 42.9%            |
| May 23 (sunny)            | 3,961,084.8                             | 2,714,829.2                     | 40.7%            |
| May 24 (cloudy and sunny) | 2,342,420.4                             | 1,710,064.8                     | 37.0%            |

### 3.5. Economic analysis

The advantages of the passive sun-tracking system on economic aspects were demonstrated based on comparisons with other reported apparatus with the similar functions. The apparatus designed by Boukdir and EL Omari [36] employed 3D printed support structure together with multiple parts, including three LDR sensors, Fresnel lenses, vacuum tube collectors, microcontrollers, RTC modules, touch screens, power modules and so on. The dual-axis solar tracker developed by Anshory et al. [39] employed the external power source to help rotating the panel support based on the ESP8266 microcontroller and the LDR sensor. Lu and Ajay [38] used two different sensors, one for sun position prediction and one for solar panel movement adjustment, to fulfill the dual axis sun tracking operation with help of the external power supply. It is concluded, therefore, the passive sun-tracking system reported in this paper show superior cost advantages based on the fact that it is built at simple mechanical structures without employing external power source and complex control systems.

**Table 3** lists the total expenses for worm gear, LDR with controller and two motors, which are the supplementary parts of the passive sun-tracking system over the fixed tilted system. The annual benefit is estimated at 35% extra daily power output (about 0.2 kWh) for 240 sunny days (accounting for approximately 65% of 365 days in Qingdao city) at electricity price of 1RMB/kWh. It is calculated, therefore, the payback period for the passive sun-tracking is about 10 years.

**Table 3.** Cost-benefit analysis.

| Cost (parts vs. prices) |         | Benefit                  |           |
|-------------------------|---------|--------------------------|-----------|
| worm gear               | 120 RMB | Daily extra power output | 0.2 kWh   |
| LDR with controller     | 250 RMB | Electricity              | 1 RMB/kWh |
| 2 motors                | 110 RMB | Annual power output days | 240       |

### 4. Conclusion

In this paper, a passive sun-tracking system was designed and fabricated. Detailed mechanical parts, the control part and the measurement unit were described. The advantages of the sun tracking system were illustrated by comparing with the power output of a fixed solar panel system. It is concluded that:

- 1) The power consumption to drive the passive sun tracking solar panel system is less than 5 W and can be well covered by the power generated by the solar panel, which is in the range of 20–100 W on a sunny day in the spring season;
- 2) Based on comparative measurement results on the power output of the sun passive tracking solar panel system and the fixed panel system at a tilting angle of 34°, it is concluded that the power generation efficiency of the passive sun tracking system is obviously higher than that of the fixed panel system, especially in the morning and afternoon of the day;
- 3) The accumulative daily power output of the solar panel in the passive sun-tracking system is 28.5%–42.9% higher than that of the fixed panel system under the sunny weather conditions. Even in the partly cloudy weather, the passive sun-tracking solar system could still generate 37% more power than the fixed panel system.

**Author contributions:** Conceptualization, YL and DD; methodology, YL and DD; formal analysis, GS and DH; investigation, GS and DH; writing—original draft preparation, GS; writing—review and editing, ZH and DD; supervision, ZH and DD; project administration, YL and DD. All authors have read and agreed to the published version of the manuscript.

**Acknowledgement:** We gratefully acknowledge the financial support of the Graduate tutor foundation of Qingdao University of Science and Technology (120202190414).

**Conflict of interest:** The authors declare no conflict of interest.

## References

1. Wang X, Cui X, Wang F, et al. Miscibility characteristics of the CO<sub>2</sub>/n-hexadecane system with presence of water component based on the phase equilibrium calculation on the interface region. *Colloids and Surfaces A: Physicochemical and Engineering Aspects*. 2021; 629: 127463. doi: 10.1016/j.colsurfa.2021.127463
2. Cui P, Liu Z, Cui X, et al. Impact of water on miscibility characteristics of the CO<sub>2</sub>/n-hexadecane system using the pendant drop shape analysis method. *Arabian Journal of Chemistry*. 2023; 16(9): 105038. doi: 10.1016/j.arabjc.2023.105038
3. Cui X, Zheng L, Liu Z, et al. Determination of the minimum miscibility pressure of the CO<sub>2</sub>/oil system based on quantification of the oil droplet volume reduction behavior. *Colloids and Surfaces A: Physicochemical and Engineering Aspects*. 2022; 653: 130058. doi: 10.1016/j.colsurfa.2022.130058
4. Du D, Sun S, Zhang N, et al. Pressure distribution measurements for co<sub>2</sub> foam flow in porous media. *Journal of Porous Media*. 2015; 18(11): 1119-1126. doi: 10.1615/jpormedia.2015012151
5. Du D, Zhang N, Li Y, et al. Parametric studies on foam displacement behavior in a layered heterogeneous porous media based on the stochastic population balance model. *Journal of Natural Gas Science and Engineering*. 2017; 48: 1-12. doi: 10.1016/j.jngse.2017.08.035
6. Du D, Zheng L, Ma K, et al. Determination of diffusion coefficient of a miscible CO<sub>2</sub>/n-hexadecane system with Dynamic Pendant Drop Volume Analysis (DPDVA) technique. *International Journal of Heat and Mass Transfer*. 2019; 139: 982-989. doi: 10.1016/j.ijheatmasstransfer.2019.05.083
7. Du D, Zhang X, Yu K, et al. Parameter Screening Study for Optimizing the Static Properties of Nanoparticle-Stabilized CO<sub>2</sub> Foam Based on Orthogonal Experimental Design. *ACS Omega*. 2020; 5(8): 4014-4023. doi: 10.1021/acsomega.9b03543
8. Li Y, Zhao D, Du D. Computational study on the three phase displacement characteristics of foam fluids in porous media.

- Journal of Petroleum Science and Engineering. 2022; 215: 110732. doi: 10.1016/j.petrol.2022.110732
9. Liu Z, Cui P, Cui X, et al. Prediction of CO<sub>2</sub> solubility in NaCl brine under geological conditions with an improved binary interaction parameter in the Søreide-Whitson model. *Geothermics*. 2022; 105: 102544. doi: 10.1016/j.geothermics.2022.102544
  10. Liu Z, Yan S, Zang H, et al. Quantization of the water presence effect on the diffusion coefficients of the CO<sub>2</sub>/oil system with the dynamic pendant drop volume analysis technique. *Chemical Engineering Science*. 2023; 281: 119142. doi: 10.1016/j.ces.2023.119142
  11. Song X, Cui X, Jiang L, et al. Multi-parameter screening study on the static properties of nanoparticle-stabilized CO<sub>2</sub> foam near the CO<sub>2</sub> critical point. *Arabian Journal of Chemistry*. 2022; 15(3): 103676. doi: 10.1016/j.arabjc.2021.103676
  12. Chong Z, Wang Q, Wang L. Is the photovoltaic power generation policy effective in China? A quantitative analysis of policy synergy based on text mining. *Technological Forecasting and Social Change*. 2023; 195: 122770. doi: 10.1016/j.techfore.2023.122770
  13. He YL, Qiu Y, Wang K, et al. Perspective of concentrating solar power. *Energy*. 2020; 198: 117373. doi: 10.1016/j.energy.2020.117373
  14. Li YG, Du DX. Characterization of Amorphous Silicon Thin Films Deposited on Upilex-s Polyimide Substrates for Application in Flexible Solar Cells. *Advanced Materials Research*. 2009; 87-88: 416-421. doi: 10.4028/www.scientific.net/amr.87-88.416
  15. Li G, Li M, Taylor R, et al. Solar energy utilisation: Current status and roll-out potential. *Applied Thermal Engineering*. 2022; 209: 118285. doi: 10.1016/j.applthermaleng.2022.118285
  16. Qiu S, Wang K, Lin B, et al. Economic analysis of residential solar photovoltaic systems in China. *Journal of Cleaner Production*. 2021; 282: 125297. doi: 10.1016/j.jclepro.2020.125297
  17. Russo MA, Carvalho D, Martins N, et al. Future perspectives for wind and solar electricity production under high-resolution climate change scenarios. *Journal of Cleaner Production*. 2023; 404: 136997. doi: 10.1016/j.jclepro.2023.136997
  18. Shahabuddin M, Alim MA, Alam T, et al. A critical review on the development and challenges of concentrated solar power technologies. *Sustainable Energy Technologies and Assessments*. 2021; 47: 101434. doi: 10.1016/j.seta.2021.101434
  19. Tang W, Qi J, Wang Y, et al. Dense station-based potential assessment for solar photovoltaic generation in China. *Journal of Cleaner Production*. 2023; 414: 137607. doi: 10.1016/j.jclepro.2023.137607
  20. Zhang X, Ang YS, Ye Z, et al. Three-terminal heterojunction bipolar transistor solar cells with non-ideal effects: Efficiency limit and parametric optimum selection. *Energy Conversion and Management*. 2019; 188: 112-119. doi: 10.1016/j.enconman.2019.03.034
  21. Zhang X, Li J, Wang J, et al. Three-dimensional Dirac material anode enables concentrated solar thermionic converters. *Optics Letters*. 2021; 46(18): 4530. doi: 10.1364/ol.434653
  22. Zhang X, Rahman E. Solar thermionic energy converters with micro-gap spacers. *Optics Letters*. 2023; 48(15): 4173. doi: 10.1364/ol.498374
  23. García-López M, Montano B, Melgarejo J. The financial competitiveness of photovoltaic installations in water utilities: The case of the Tagus-Segura water transfer system. *Solar Energy*. 2023; 249: 734-743. doi: 10.1016/j.solener.2022.12.025
  24. Palm J. Household installation of solar panels – Motives and barriers in a 10-year perspective. *Energy Policy*. 2018; 113: 1-8. doi: 10.1016/j.enpol.2017.10.047
  25. Yao H, Zhou Q. Research status and application of rooftop photovoltaic Generation Systems. *Cleaner Energy Systems*. 2023; 5: 100065. doi: 10.1016/j.cles.2023.100065
  26. Imteaz MA, Ahsan A. Solar panels: Real efficiencies, potential productions and payback periods for major Australian cities. *Sustainable Energy Technologies and Assessments*. 2018; 25: 119-125. doi: 10.1016/j.seta.2017.12.007
  27. Widodo Besar Riyadi T, Effendy M, Radiant Utomo B, et al. Performance of a photovoltaic-thermoelectric generator panel in combination with various solar tracking systems. *Applied Thermal Engineering*. 2023; 235: 121336. doi:

- 10.1016/j.applthermaleng.2023.121336
28. Mamodiya U, Tiwari N. Dual-axis solar tracking system with different control strategies for improved energy efficiency. *Computers and Electrical Engineering*. 2023; 111: 108920. doi: 10.1016/j.compeleceng.2023.108920
  29. Zhu Y, Liu J, Yang X. Design and performance analysis of a solar tracking system with a novel single-axis tracking structure to maximize energy collection. *Applied Energy*. 2020; 264: 114647. doi: 10.1016/j.apenergy.2020.114647
  30. Mpodi EK, Tjiparuro Z, Matsebe O. Review of dual axis solar tracking and development of its functional model. *Procedia Manufacturing*. 2019; 35: 580-588. doi: 10.1016/j.promfg.2019.05.082
  31. Josely Jose P, Akbari P, Dhokiya J, et al. Solar tracking: The best alternative to obtain more solar power output. *Materials Today: Proceedings*. 2022; 67: 921-926. doi: 10.1016/j.matpr.2022.08.065
  32. Zaghba L, Khennane M, Mekhilef S, et al. Experimental outdoor performance assessment and energy efficiency of 11.28 kWp grid tied PV systems with sun tracker installed in saharan climate: A case study in Ghardaia, Algeria. *Solar Energy*. 2022; 243: 174-192. doi: 10.1016/j.solener.2022.07.045
  33. Muthukumar P, Manikandan S, Muniraj R, et al. Energy efficient dual axis solar tracking system using IOT. *Measurement: Sensors*. 2023; 28: 100825. doi: 10.1016/j.measen.2023.100825
  34. Ravikiran Ch, Nagaraju S, Akhil D, et al. Design of solar array with sun position tracking system employing refrigerant. *Materials Today: Proceedings*. doi: 10.1016/j.matpr.2023.05.032
  35. Awasthi A, Shukla AK, S.R. MM, et al. Review on sun tracking technology in solar PV system. *Energy Reports*. 2020; 6: 392-405. doi: 10.1016/j.egy.2020.02.004
  36. Boukdir Y, EL Omari H. Novel high precision low-cost dual axis sun tracker based on three light sensors. *Heliyon*. 2022; 8(12): e12412. doi: 10.1016/j.heliyon.2022.e12412
  37. Palomino-Resendiz SI, Flores-Hernández DA, Cantera-Cantera LA, et al. Design and implementation of Model-Based Predictive Control for two-axis Solar Tracker. *Solar Energy*. 2023; 265: 112080. doi: 10.1016/j.solener.2023.112080
  38. Lu W, Ajay P. Solar PV tracking system using arithmetic optimization with dual axis and sensor. *Measurement: Sensors*. 2024; 33: 101089. doi: 10.1016/j.measen.2024.101089
  39. Anshory I, Jamaaluddin J, Fahrudin A, et al. Monitoring solar heat intensity of dual axis solar tracker control system: New approach. *Case Studies in Thermal Engineering*. 2024; 53: 103791. doi: 10.1016/j.csite.2023.103791
  40. Kumar Gupta A, Kumar Chouksey V, Pandey A. Design and study of an autonomous linear welding robot with mechanical referencing system. *Materials Today: Proceedings*. Published online August 2023. doi: 10.1016/j.matpr.2023.08.111
  41. Xu L, Ding P, Zhang Y, et al. Sensitivity analysis of the shading effects from obstructions at different positions on solar photovoltaic panels. *Energy*. 2024; 290: 130229. doi: 10.1016/j.energy.2023.130229
  42. Zhou X, Duan Z. Investigation on the basic principles of human-machine contact force, based on screw theory. *Heliyon*. 2023; 9(3): e13851. doi: 10.1016/j.heliyon.2023.e13851
  43. Alomar OR, Ali OM, Ali BM, et al. Energy, exergy, economical and environmental analysis of photovoltaic solar panel for fixed, single and dual axis tracking systems: An experimental and theoretical study. *Case Studies in Thermal Engineering*. 2023; 51: 103635. doi: 10.1016/j.csite.2023.103635